Int J Adv Manuf Technol (2016) 82:2065–2073
DOI 10.1007/s00170-015-7515-2

ORIGINAL ARTICLE

Motion straightness of hydrostatic guideways considering the ratio of pad center spacing to guide rail profile error wavelength

Jun Zha[1] · **Dun Lv**[1] · **Qian Jia**[1] · **Yaolong Chen**[1]

Received: 12 December 2014 / Accepted: 30 June 2015 / Published online: 16 July 2015

Abstract Due to the error averaging effect of pressured oil film in hydrostatic guideways, motion straightness of the slider is smaller than the profile error of guide rails. In spite of this, structural parameters of the guideway system have dramatic effects on the error averaging coefficient. Therefore, it is necessary to investigate the relationship between the structural parameters of the guideway system and slider motion straightness. In this paper, effect of the ratio (m_λ) of pad center spacing to guide rail profile error wavelength on motion straightness was the primary focus. A static analysis model based on the error averaging effect considering pad center spacing in open hydrostatic guideways with four pads was established. Linear displacement motion error of the slider with different system structural parameters was solved, and slider motion straightness was calculated using least-square method. A grinding machine LGF1000 was used in experiments, and the slider vertical motion straightness was improved to 0.98 μm/600 mm from 2.08 μm/600 mm after using the lapping process on a specific guide rail along the *Y*-axis for change the m_λ. In addition, precision was improved by 52.9 %. Results show that m_λ has significant influence on vertical motion straightness of the slider. Increasing the pad center spacing m allows a reduction in motion straightness for m_λ equal or lesser than 0.5. However, a decrease in the pad center spacing is useful to decrease the motion straightness, when m_λ is equal or larger than 0.72.

✉ Yaolong Chen
chenzwei@mail.xjtu.edu.cn

[1] State Key Laboratory for Manufacturing Systems Engineering, Xi'an Jiaotong University, 28 Xianning Road, Xi'an 710049, People's Republic of China

Keywords Hydrostatic guideways · Error averaging · Motion straightness · Pad center spacing · Precision design

1 Introduction

Hydrostatic guideways are widely used as a vital functional unit in ultra-precision machine tools and coordinate measuring machines [1–5]. The motion straightness directly influences accuracy of the machined or measured parts [6]. The use of pressured oil film in hydrostatic guideways results in an averaging effect on the errors. Due to this averaging, motion straightness of the slider is smaller than the profile error of guide rails [7–9]. In addition, structural parameters of the slider such as pad length to width ratio, number of pads, and their configuration have an important impact on motion straightness [10]. In order to improve motion straightness of the slider used in hydrostatic guideways, the effect of error averaging should be used as an advantage to conduct and guide precision design of hydrostatic guideways systems.

Over the recent decades, substantial research on the relationship between guide rail profile error and motion straightness of a slider to study error averaging has been carried out. Yabe et al. [11] studied the relationship between the sliding accuracy of an externally pressurized gas lubricated pad bearing and machining error of the guide rail. They found that the accuracy was related to the ratio of guide rail profile error wavelength to pad length. Shamoto et al. [12] investigated the relationship between action force of the film on a single pad and the geometric error of a guide rail at various spatial frequencies using finite element analysis. They decreased profile error by lapping rail surfaces, which resulted in improved motion straightness. Park et al. [13, 14] determined the transfer function for a single pad and proposed a machining algorithm based on reverse analysis to improve motion accuracy

for hydrostatic table. Ekinci et al. [15, 16] analyzed motion errors in aerostatic guideways based on geometric relationship and static equilibrium. Based on this analysis, they established a model for the quantitative estimation of motion accuracy. Xue et al. [17] established a static analysis model to determine theoretical motion error for closed hydrostatic guideways with four pads, the effects of some design parameters on error averaging effect were researched respectively, and some suggestions to improve the precision in design were proposed. However, the parameters matching of hydrostatic guideways, as the relationship between slider structural parameter and guide rail profile errors, which affect motion straightness, needs further research at the present stage.

A common approach to improve motion straightness of a slider is to reduce profile error of the guide rails using the manual lapping machining process. Shamoto et al. proposed a method to improve guide rails using a transfer function model, which allows the determination of the error averaging coefficient. After which, a reverse analysis approach based on the measured error and lapping information can be used to estimate the profile error for the guide rails [18, 19]. Hwang et al. [20] estimated motion errors for *X*- and *Y*-stages using the static equilibrium of an aerostatic bearing obtained from the measured profile errors for the guide rails. Similarly, motion straightness for rolling guides can be improved by lapping the guide rails [21]. However, for this situation, motion straightness should be estimated repeatedly after the lapping machining processes until the precision requirements are met.

The lapping process for the guide rails alters the relationship between various system structural parameters and decreases the error averaging coefficient. However, it is important to note there are a few quantitative analysis reports specific to this area and a more detailed analysis is required. Motion straightness is typically considered as zero when the ratio of pad center spacing to profile error wavelength of guide rails is equal to 0.5, 1.5, 2.5… [15]. However, in real applications, the ratio m_λ of pad center spacing m to profile error wavelength of guide rails λ cannot achieve the abovementioned specific values and for most cases it is located in one of the intervals. For this reason, we need to investigate the influence of m_λ on motion straightness and provide theoretic guidelines for precision design of hydrostatic guideways. Based on our previous research, a static analysis model considering pad center spacing and guide rail profile error in open hydrostatic guideways is proposed in this study. The influence of m_λ on motion straightness is investigated. Experiments were used to measure motion straightness of the slider after the value of m_λ changed, which allowed the verification of the accuracy of the proposed model.

2 Hydrostatic guideway static analysis model considering pad center spacing

2.1 Model and assumption

For mathematical description of the guide rail profile error, let us assume that the error along the width direction of the pads does not change. So, profile error for the guide rails can be fitted by Fourier series, and the function representing the profile error can be expressed as $f_z(y)=E\sin(2\pi/\lambda\cdot y+\varphi)$ [7], where E, λ, and φ are amplitude, wavelength, and phase angle of guide rail profile error, respectively.

For open hydrostatic guideways, slider-guide rail structure can be simplified as the model shown in Fig. 1, where pad 1 and pad 2 are marked numerically as 1 and 2, m is the spacing between the centers of pad 1 and pad 2, $e_z(y)$ is linear displacement motion error of the slider, and λ is the profile error wavelength of the guide rail.

2.2 Static analysis of open hydrostatic guideways with four pads

2.2.1 Oil film thickness calculation method considering guide rail profile error

A pad advancing along the *Y* direction is shown in Fig. 2. Plane *xOy* denotes a perfect guide rail without errors. $z=f_z(y)$ is the function of the actual guide rail with profile error. Assuming that the profile error does not change along the width direction of the pad, oil film thickness of the land at any coordinate is given by $h(y)=h_0-f_z(y)$.

The oil film of the land along the y direction is divided into N equal elements with length b_w, and A_i is the area of the ith element. Total area of land oil film is A. For the original point o' located at an arbitrary coordinate, the corresponding coordinate of the ith element is y_i and $h(y_i)$ is the oil film thickness for this element. Therefore, average oil film thickness for the whole land is given as

$$h_a(y) = \frac{1}{A}\sum_{i=1}^{N} h(y_i)A_i \tag{1}$$

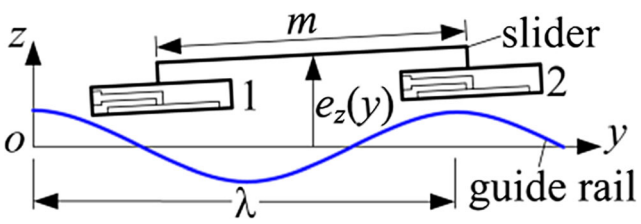

Fig. 1 Simplified schematic of a slider-guide rail

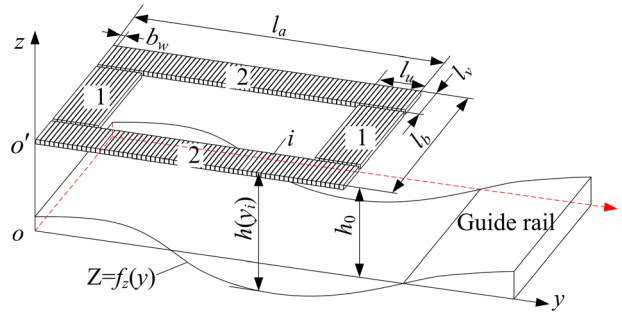

Fig. 2 Guide rail profile error and pad structure. *1* oil film along width direction, *2* oil film along length direction, l_a pad length, l_u land width along pad length direction, l_b pad width, l_v land width along pad width direction, b_w discrete unit width of oil film, h_0 nominal oil film thickness, $f_z(y)$ guide rail profile error function

When o' moves, Δy is the displacement along the y direction, and volume variations of the oil film 1 and 2 are ΔV_1 and ΔV_2, respectively. From coordinate y_1 to y_2, the variation of average oil film thickness is given as

$$\Delta h_a = \frac{1}{A}\left(\int_{y_1}^{y_2}\Delta V_1 + \int_{y_1}^{y_2}\Delta V_2\right) \tag{2}$$

Therefore, average oil film thickness for the whole land of a single pad at coordinate y is represented by

$$h_a(y) = h_a(0) + \Delta h_a|_0^y \tag{3}$$

2.2.2 Calculation method of oil film reaction force variation

The pressured oil in the pad can be assumed to be an incompressible Newtonian fluid with a constant viscosity, and the oil supply pressure can be considered as a constant value. The flow between the land and the guide rail is assumed as a Poiseuille flow [10]. The nominal oil film thickness $h(y)$ can be substituted by the average oil film thickness. Thus, flow resistance for the whole land is given as,

$$R(y) = \frac{3\eta}{h_a(y)^3((l_a - l_u)/4l_v + (l_b - l_v)/4l_u)} \tag{4}$$

When resistance of the restrictor is $R_c(y)$, oil pressure in the pocket of the pad is

$$p_0(y) = \frac{p_s}{R_c(y)/R(y) + 1} \tag{5}$$

Therefore, the variation of film reaction force from the original point to coordinate y is

$$f_e(y) = (p_0(y) - p_0(0))A_e \tag{6}$$

where A_e is the loading area of the oil film.

2.2.3 Calculation of oil film force considering guide rail profile error and pad center spacing

Profile error functions for the two guide rails below pad 1 and pad 2 and below pad 3 and pad 4 are represented as $z=f_{z1}(y)$ and $z=f_{z2}(y)$, respectively. With pressured oil being supplied, an equivalent static model can be used to describe the open hydrostatic guideways with four pads, as shown in Fig. 3. Pads in the horizontal direction were not contained.

The oil film in the hydrostatic guideways is simplified as a linear spring element, so the oil film balance force is given as

$$\begin{aligned} f_{bj}(y) &= f_j(y) - f_{ej}(y) \\ &= -k_j(y)\cdot\left[a_j e_z(y) + b_j\theta_x\cdot\frac{m}{2} + c_j\theta_y\cdot\frac{n}{2}\right] \end{aligned} \tag{7}$$

where $e_z(y)$ is the line displacement motion error of the slider in Z direction, θ_x is the pitch angular deviation, θ_y is the roll angular deviation, $f_{ej}(y)$ is the variation of film reaction force for the jth pad when slider advances along Y direction, $f_{bj}(y)$ is the balance force for the jth pad, and a_j, b_j, and c_j are direction coefficients (j=1 ~ 4), a=(1,1,1,1), b=(1,−1,1,−1), and c=(1,1,−1,−1).

2.3 Calculating the slider linear displacement motion error

The resultant force and moment of the slider must zero when the slider moves to any coordinate. The force equilibrium equation and the moment equilibrium equation are expressed as

$$\begin{cases} \sum_{j=1}^{4} a_j f_j(y) - G - W = 0 \\ M_x = 0 \Rightarrow \sum_{j=1}^{4} b_j f_j(y)\frac{m}{2} + W\cdot m_1 = 0 \\ M_y = 0 \Rightarrow \sum_{j=1}^{4} c_j f_j(y)\frac{n}{2} - W\cdot n_1 = 0 \end{cases} \tag{8}$$

Substitute Eq. (7) with Eq. (8) and e_z is solved as

$$e_z = A_1\cdot\left(\sum_{j=1}^{4} a_j F_{ej} - G - W, \sum_{j=1}^{4} b_j F_{ej}, \sum_{j=1}^{4} c_j F_{ej}\right)^{\mathrm{T}} \tag{9}$$

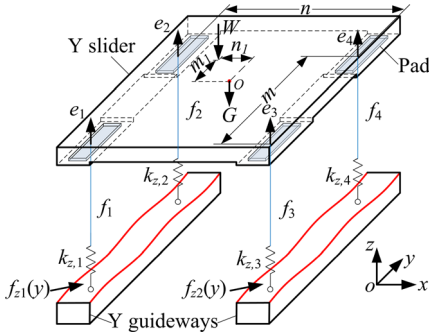

Fig. 3 Open hydrostatic guideways equivalent mechanical model. $k_{z1}(y) \sim k_{z4}(y)$ oil film stiffness of pads, $e_1(y) \sim e_4(y)$ line motion error at pad centers, $f_1(y) \sim f_4(y)$ pad reaction force, m pad center spacing along Y direction, n pad center spacing along X direction, G dead load of slider, W load of working position, m_1 the distance between working position and slider center along Y direction, n_1 the distance between working position and slider center along X direction

where A is the oil film stiffness coefficient matrix, A^- is the inverse matrix of A. A_1, A_2, and A_3 are row vectors of matrix A^-.

$$A = \begin{bmatrix} \sum_{j=1}^{4} a_j^2 k_j & \sum_{j=1}^{4} a_j b_j k_j & \sum_{j=1}^{4} a_j c_j k_j \\ \sum_{j=1}^{4} a_j b_j k_j & \sum_{j=1}^{4} b_j^2 k_j & \sum_{j=1}^{4} b_j c_j k_j \\ \sum_{j=1}^{4} a_j c_j k_j & \sum_{j=1}^{4} b_j c_j k_j & \sum_{j=1}^{4} c_j^2 k_j \end{bmatrix}, \quad A^- = \begin{bmatrix} A_1 \\ A_2 \\ A_3 \end{bmatrix}$$

3 Experimental method

3.1 Experimental setup

The structure of the experimental setup is shown in Fig. 4. Y-axis is composed of open hydrostatic guideways, which have four pads in the vertical direction and two pairs of opposed pads in the horizontal direction. The Y guide rails are made of nature granite.

Parameters for the experimental setup, which contain the guide rail, oil supply system, and fixed restrictor, are listed in Table 1. An annular slit fixed restrictor is used in the open hydrostatic guideways [7, 22, 23].

3.2 Guide rails with different profile errors

The value of pad center spacing m remains unchanged in the setup. This experiment aims at one part of the whole guide rail of Y-axis. Guide rails 1, 2, and 3 with different profile error wavelengths were obtained using the lapping machining process. The wavelengths for guide rails 1, 2, and 3 are λ_1, λ_2, and λ_3, respectively. It can be seen from Fig. 5 that the three guide rails have the same length. The $\lambda_1{:}\lambda_2{:}\lambda_3 = 3{:}2{:}1$, so $m/\lambda_1{:}m/\lambda_2{:}m/\lambda_3 = 1{:}2{:}3$. The oil film thickness h_0 remains unchanged for comparing slider motion straightness on three guide rails with different profile errors.

The three guide rails shown in Fig. 5 were specific part of Y guide rails, as shown in Fig. 6. Wherein, guide rail 1 is the original condition. Guide rails 2 and 3 were conditions after the first and the second lapping machining processes conducted on guide rail 1, respectively.

3.3 Measurement of motion straightness

Pad center spacing was 0.94 m along the Y direction. The Y slider moved with a stroke of 1260 mm and ran at a speed of 1 m/min. The measuring environmental conditions were as follows: room temperature was controlled within 21±0.1 °C, the humidity was 45.4 %, and experimental setup stood on a 3-m-thick concrete floor with an isolation trench. A picture of the experimental setup is shown in Fig. 7. The experimental setup used here was a grinding machine LGF1000. The machine base and X/Y-axis were made of nature granite. Y-axis was gantry type and employed open hydrostatic guideways with four pads in the vertical direction. The X beam was used as Y slider. X slider and Z axis are integrated together. To compare the variations in motion straightness of the slider with different guide rail profile error wavelengths, Y slider vertical motion straightness was measured using a laser interferometer XL80 (contains Laser head, Straightness interferometer, and Reflector) to verify the influence of m_λ on motion straightness.

For ease of comparison between the measured results for different guide rails, the least square line of the measured data was rotated to be coaxial with the horizontal axis. Spacing between the envelope lines through the highest point and lowest point is the motion straightness error.

4 Results and discussions

4.1 Comparison between theoretical and experimental results

Under initial conditions, vertical motion straightness of the slider along the Y-axis is 3.91 μm/1260 mm. Line

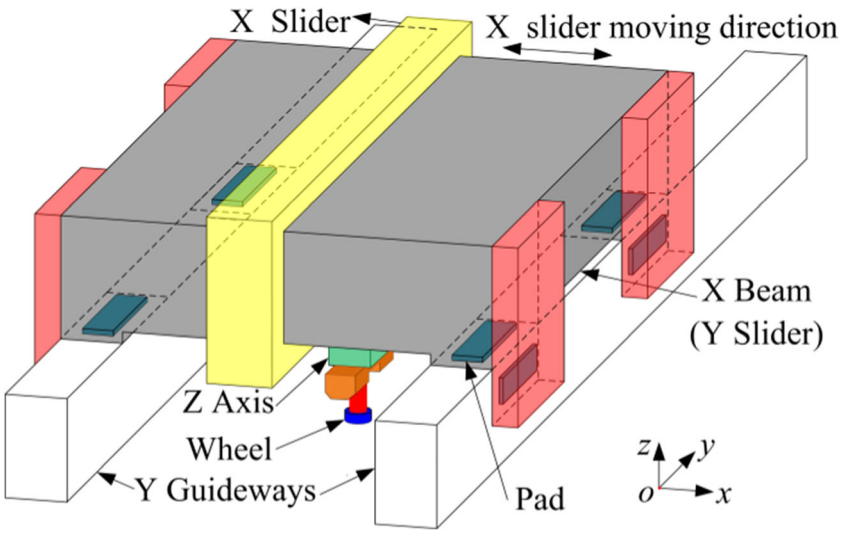

Fig. 4 Experimental setup structural schematic

displacement motion error of the slider is shown in Fig. 8. It can be seen that line displacement motion error of the slider has large fluctuations within the stroke of 80~680 mm of the guide rail. For this part of the whole guide rail of *Y*-axis as guide rail 1, the corresponding vertical motion straightness is 2.08 μm/600 mm.

Following the lapping machining processes as described in the "Guide rails with different profile errors" section, the profile error of guide rail 1 is changed. This changed guide rail is now considered as guide rail 2. The corresponding vertical motion straightness of the *Y*-axis slider is 1.33 μm/600 mm (red curve in Fig. 9). The slider vertical motion straightness for guide rail 2 shows a 36.1 % increase in precision compared to guide rail 1. Slider vertical motion straightness was 2.85 μm/1260 mm for a full stroke along the *Y*-axis and shows a 27.1 % increase in precision.

Lapping was repeated for both ends of guide rail 2, and guide rail 3 was obtained. The slider vertical motion straightness for guide rail 3 was 0.98 μm/600 mm (blue curve in Fig. 9), which shows a 52.9 % increase in precision compared to guide rail 1. Correspondingly, the slider vertical motion straightness was 1.01 μm/1260 mm for a full stroke along the *Y*-axis (blue curve in Fig. 10). The experimental results indicate that the precision of the slider vertical motion straightness for full-stroke 3 (contains guide rail 3) increased by 74.2 and 64.6 % in comparison to full-stroke 1 (contains guide rail 1) and full-stroke 2 (contains guide rail 2), respectively.

Based on the model discussed in the "Hydrostatic guideway static analysis model considering pad center spacing" section, linear displacement motion error of the slider at any coordinate was obtained using Eq. (9). The obtained motion error was fitted using the least-square method, and vertical motion straightness of the slider was calculated. After measuring the slider vertical motion straightness, parameters containing profile error amplitude and wavelength of the guide rails were calculated. The amplitude and first-order wavelength of the guide rail profile error are approximately 5 μm and 1.2 m, respectively.

Table 1 Experimental setup parameters

Parameter	Value	Parameter	Value
Dead load of *Y* slider/*N*	40,000	Land width (length direction) l_u/mm	50
Dead load of *X* slider and *Z*-axis/*N*	14,960	Land width (width direction) l_v/mm	27.5
Pad center spacing along *X*-axis/m	2.55	Nominal oil film thickness h_0/μm	20
Pad center spacing along *Y*-axis/m	0.94	Oil supply pressure P_s/Mpa	1.4
Y slider stroke/mm	1260	Oil dynamic viscosity η/Pa.s	0.0615
Pad length l_a/mm	400	Restrictor throttle length/mm	8.9
Pad width l_b/mm	80	Restrictor throttle gap/μm	40

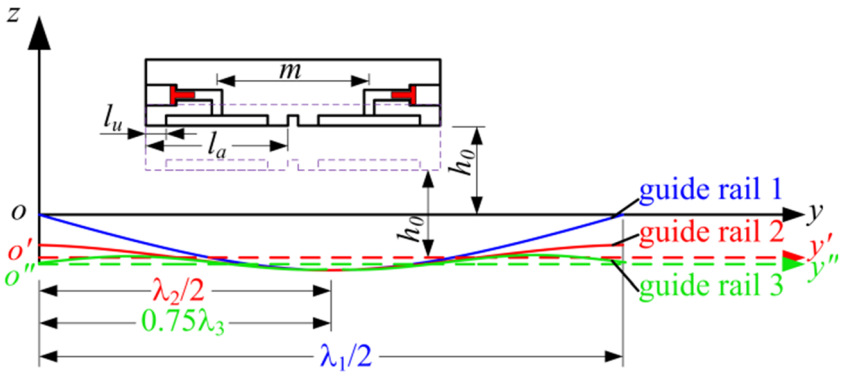

Fig. 5 Three guide rails with different profile error wavelengths

Error averaging coefficient n_e was defined as the ratio of vertical motion straightness to the guide rail profile error amplitude, and n_λ is defined as the ratio of the pad length l_a to the guide rail profile error wavelength. The relationship between n_e and n_λ for an evaluation length, 600 mm, is shown in Fig. 11. For n_λ(=0.4/1.2) in guide rail 1, the corresponding n_e is 0.430 (red dotted line in Fig. 11). For n_λ(=0.4/0.6) in guide rail 2, the corresponding n_e is 0.051 (grey dotted line in Fig. 11). For n_λ(=0.4/0.4) in guide rail 3, the corresponding n_e is 0.002 (blue dotted line in Fig. 11). The theoretical vertical motion straightness of the *Y*-axis slider on guide rails 1, 2, and 3 are 2.15 μm/600 mm, 0.26 μm/600 mm, and 0.01 μm/600 mm, respectively. However, the experimental vertical motion straightness of the *Y*-axis slider on guide rails 1, 2, and 3 were 2.08 μm/600 mm, 1.33 μm/600 mm, and 0.98 μm/600 mm, and the corresponding error averaging coefficients n_e were 0.417 (red solid line in Fig. 11), 0.266 (grey solid line in Fig. 11), and 0.196 (blue solid line in Fig. 11), respectively.

The actual profile error wavelengths of guide rails 2 and 3 were larger than the theoretical value. Consequently, n_λ is smaller, but the corresponding n_e is larger than the theoretical value. This implies that the measured vertical motion straightness is larger than theoretical value. This is mainly because the manual lapping process cannot be precisely controlled. Based on the curve in Fig. 11, actual profile error wavelengths of three guide rails can be calculated as 1.21, 0.69, and 0.60 m.

4.2 The relationship between m_λ and n_e

In the "Comparison between theoretical and experimental results" section, as guide rail profile error wavelength changed, the variation in *Y* slider vertical motion straightness can be observed distinctively. For constant pad center spacing, the motion straightness can be improved significantly after the guide rail profile error wavelength was decreased. But both the pad center spacing and guide rail profile error wavelength have an effect on m_λ. So in the structural design process of *Y* slider, the pad center spacing should be optimized after the precision of guide rail was designed. In Fig. 12, the relationship between three different pad center spacing and n_e was shown. The three pad center spacing are 0.74, 0.94, and

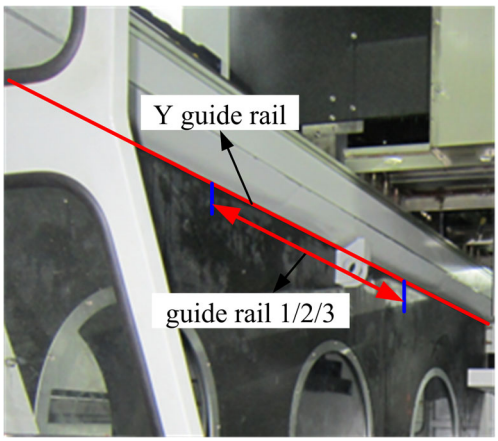

Fig. 6 *Y*-axis guide rail

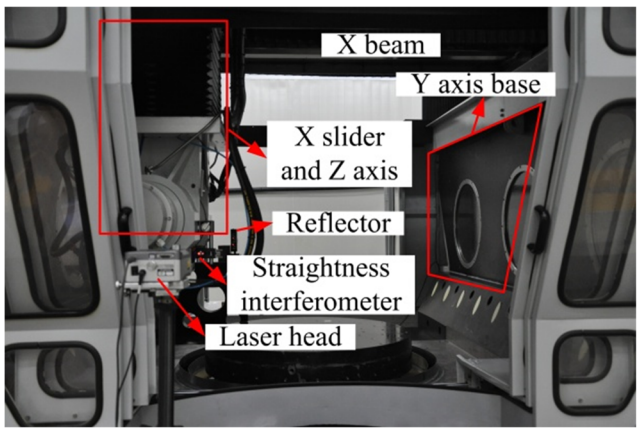

Fig. 7 Picture of experimental setup

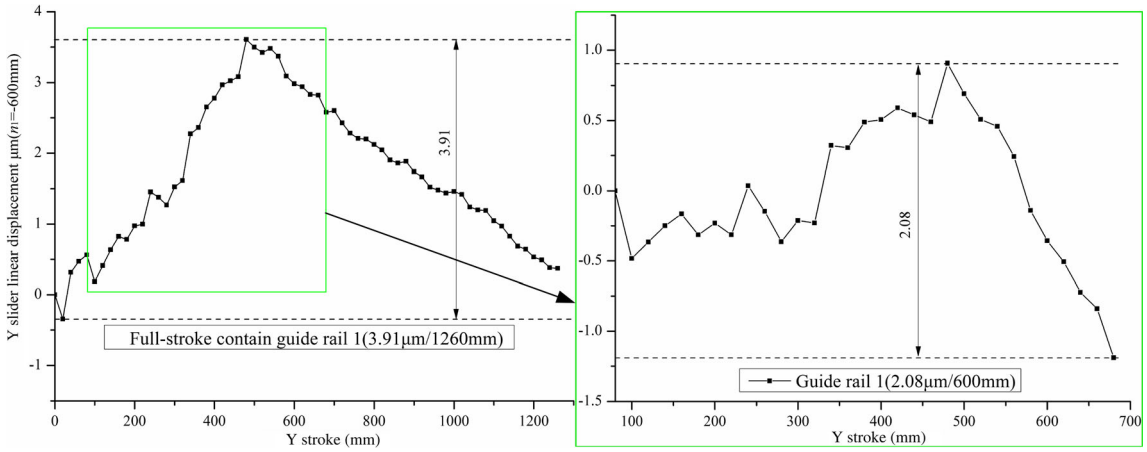

Fig. 8 Vertical motion straightness of the *Y*-axis slider within the full stroke and guide rail 1

1.14 m, and the corresponding values of m_λ are 0.72, 0.75, and 0.77, when the maximum value of error averaging coefficients is reached. It can be found that the larger the value of m, the larger is the maximum value of n_e, with a larger value for the corresponding m_λ. However, this increasing trend is not obvious. From the results in Fig. 12, it can be observed that increasing the pad center spacing is beneficial allowing a decrease in n_e when m_λ is equal or lesser than 0.5, but the extent of this decrease was limited. In addition, decreasing pad center spacing is useful to decrease n_e, when m_λ is equal to or larger than 0.72. The error averaging coefficient curve increases significantly and sharply when $0.5 \leq m_\lambda \leq 0.72$. So, m_λ should not be located within this specific interval. As m_λ is equal to 0.5, 1.5, or 2.5, the local minimum value of n_e can be reached which almost equals to zero. For the hydrostatic guideways in LGF1000, the structural parameters of the pad can be designed after the external load is confirmed. In addition, since the structural parameters of *Z*-axis are known, the value of m has been characterized. Therefore, n_e can be improved through altering the ratio of pad center spacing to guide rail profile error wavelengths.

5 Conclusions

Effect of the ratio of pad center spacing to guide rail profile error wavelength on the vertical motion straightness of the *Y*-axis slider was investigated in this study. Precision guidelines for open hydrostatic guideways are outlined. The conclusions are as follows:

1. Ratio of pads centers spacing to guide rail profile error wavelength has significant influence on vertical motion straightness of the slider. When m_λ is equal

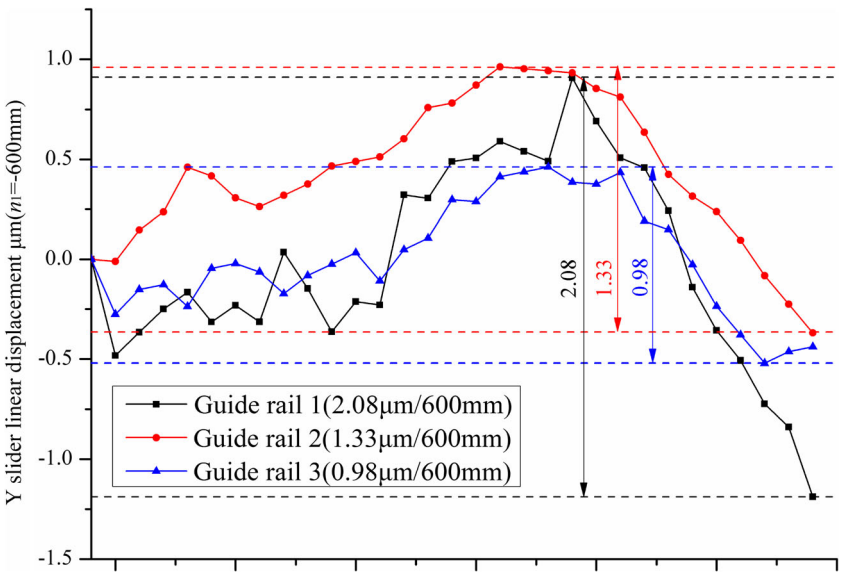

Fig. 9 *Y*-axis slider vertical motion straightness on guide rails 1, 2, and 3

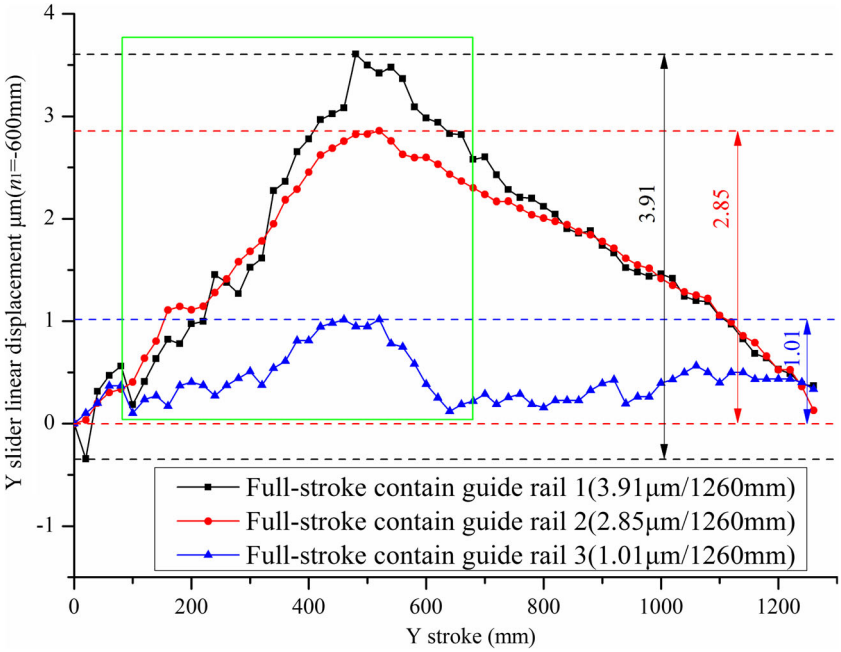

Fig. 10 *Y*-axis slider vertical motion straightness within the full stroke

or lesser than 0.5, an increase in the value of m improves the vertical motion straightness, whereas a decrease in the value of m reduced vertical motion straightness when m_λ is equal or larger than 0.72.

2. Error averaging coefficient curve increases sharply as $0.5 \leq m_\lambda \leq 0.72$. Due to this, the value of m_λ should be designed carefully to avoid this specific interval.
3. For values of m_λ equal to 0.5, 1.5, or 2.5, n_e is almost equal to zero. The results are consistent with reference [15] and validate accuracy of the model proposed in this study.
4. The slider vertical motion straightness on specific parts of the guide rail of the *Y*-axis was improved after using the lapping process. This aided in significantly improving the slider vertical motion straightness within the full stroke.

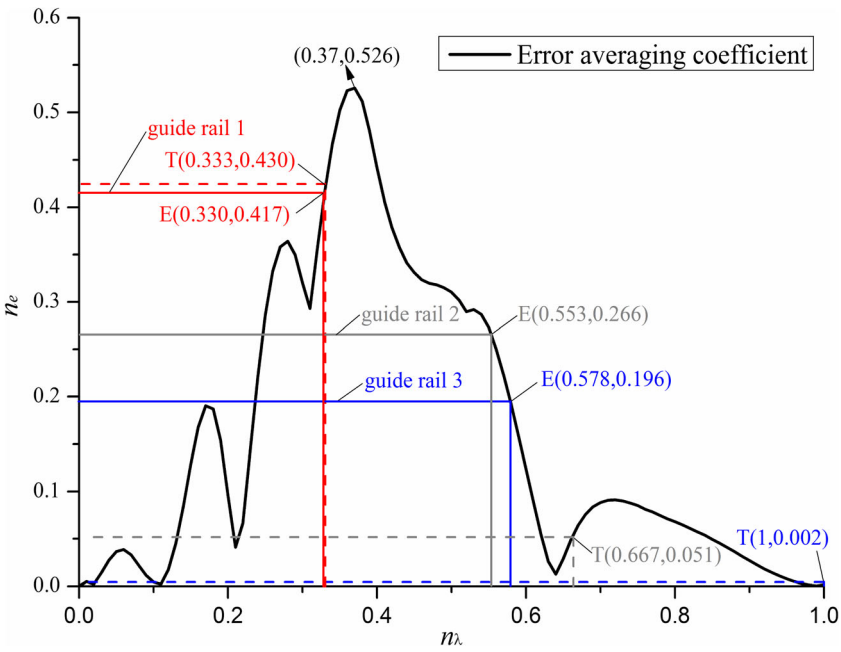

Fig. 11 Relationship between n_e and n_λ

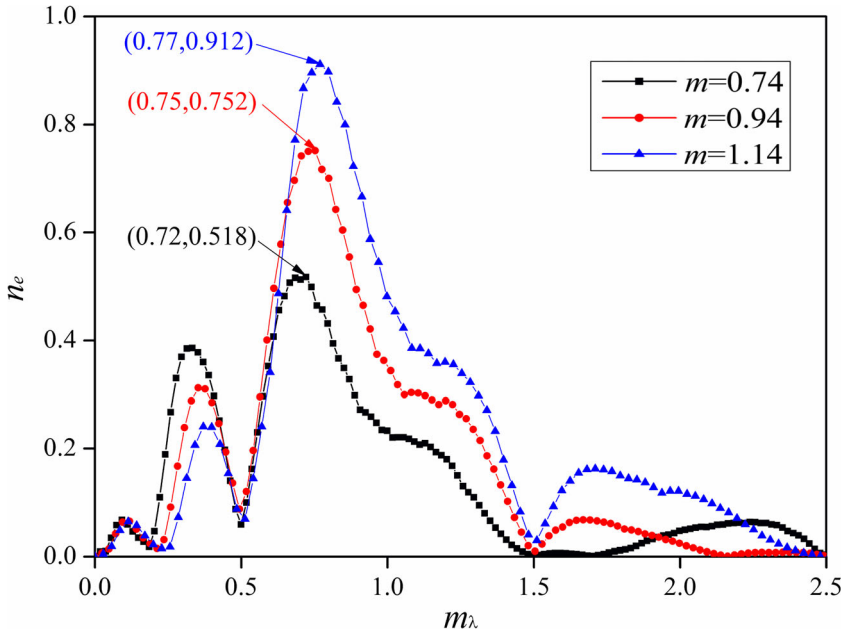

Fig. 12 Relationship between m_λ and n_e

Acknowledgments This work was supported by the National Natural Science Foundation of China (NSFC 51275395) and the National Science and Technology Major Project of the Ministry of Science and Technology of China (2012ZX04002-091).

References

1. Liu T, Gao WG, Tian YL, Mao K, Pan GX, Zhang DW (2015) Thermal simulation modeling of a hydrostatic machine feed platform. Int J Adv Manuf Technol. doi:10.1007/s00170-015-6881-0
2. Liang YC, Chen WQ, Sun YZ, Luo XC, Lu LH, Liu HT (2014) A mechanical structural-based design method and its implementation on a fly-cutting machine tool design. Int J Adv Manuf Technol 70(9-12):1915–1921
3. Schellekens P, Rosielle N, Vermeulen H, Vermeulen M, Wetzels S, Pril W (1998) Design for precision: current status and trends. Ann CIRP - Manuf Technol 47(2):557–586
4. Altintas Y, Verl A, Brecher C, Uriarte L, Pritschow G (2011) Machine tool feed drives. Ann CIRP - Manuf Technol 60(2):779–796
5. Hwang J, Park CH, Gao W, Kim S-W (2007) A three-probe system for measuring the parallelism and straightness of a pair of rails for ultra-precision guideways. Int J Mach Tools Manuf 47(7–8):1053–1058
6. Chen WQ, Lu LH, Yang K, Huo DH, Hao S, Zhang QC (2015) A novel machine tool design approach based on surface generation surface generation simulation and its implementation on a fly cutting machine tool. Int J Adv Manuf Technol. doi:10.1007/s00170-015-7058-6
7. Wang ZW, Zhao WH, Chen YL, Lu BH (2013) Prediction of the effect of speed on motion errors in hydrostatic guideways. Int J Mach Tools Manuf 64(4):78–84
8. Slocum AH, Scagnetti PA, Kane NR, Brunner C (1995) Design of self-compensated, water-hydrostatic bearings. Precis Eng 17(3):173–185
9. Kane NR, Sihler J, Slocum AH (2003) A hydrostatic rotary bearing with angled surface self-compensation. Precis Eng 27(2):125–139
10. Slocum AH (1992) Precision machine design. Dearborn, Michigan
11. Yabe H, Ikuno Y (1996) A study on sliding accuracy characteristics of an externally pressurized gas-lubricated guide way: fundamental sliding accuracy characteristics. JSME Int J Ser C 39(2):371–377
12. Shamoto E, Park CH, Moriwaki T (2001) Analysis and improvement of motion accuracy of hydrostatic feed table. Ann CIRP - Manuf Technol 50(1):285–290
13. Park CH, Oh YJ, Lee CH, Hong JH (2003) Experimental verification on the motion error analysis method of hydrostatic bearing tables using a transfer function. Int J KSPE 4(2):57–63
14. Park CH, Oh YJ, Lee CH, Hong JH (2003) Theoretical verification on the motion error analysis method of hydrostatic bearing tables using a transfer function. Int J KSPE 4(2):64–70
15. Ekinci TO, Mayer JRR (2007) Relationships between straightness and angular kinematic errors in machines. Int J Mach Tools Manuf 47(12–13):1997–2004
16. Ekinci TO, Mayer JRR, Cloutier GM (2009) Investigation of accuracy of aerostatic guideways. Int J Mach Tools Manuf 49(6):478–487
17. Xue F, Zhao WH, Chen YL, Wang ZW (2012) Research on error averaging effect of hydrostatic guideways. Precis Eng 36(1):84–96
18. Park CH, Lee CH, Lee H (2004) Corrective machining algorithm for improving the motion accuracy of hydrostatic bearing tables. Int J Precis Eng Manuf 5(2):60–67
19. Park CH, Lee CH, Lee H (2004) Experimental verification on the corrective machining algorithm for improving the motion accuracy of hydrostatic bearing table. Int J Precis Eng Manuf 5(3):62–68
20. Hwang J, Park CH, Kim SW (2010) Estimation method for errors of an aerostatic plannar XY stage based on measured profiles errors. Int J Adv Manuf Technol 46(9–12):877–883
21. Khim G, Park CH, Shamoto E, Kim SW (2011) Prediction and compensation of motion accuracy in a linear motion bearing table. Precis Eng 35(3):393–399
22. Zhao WH, Chen YL, He ZY, Wang ZW, Xue F, Lu BH (2010) Chinese Patent No. ZL201010102089.4
23. Wang ZW, Zhao WH, Li BQ, Xue F, Chen YL, Lu BH (2010) Study on static characteristics and errors of new kind of annular gap restrictor. CIRP 2nd ICPMI, Vancouver, Canada